ARCHIVES OF ACOUSTICS
18, 4, 553–575 (1993)

BIAS AND STANDARD DEVIATION OF DIGITAL MEAN AND MAXIMUM DOPPLER FREQUENCY ESTIMATORS

K. MARASEK AND A. NOWICKI

Institute of Fundamental Technological Research
Polish Academy of Sciences
(00-049 Warszawa, Świętokrzyska 21)

The performance of four spectral techniques (FFT, AR Burg, ARMA and Arithmetic Fourier Transform AFT) for mean and maximum frequency estimation of the Doppler spectra is described. The mean frequency was computed as the first spectral moment of the spectrum with and without the noise subtraction. Different definitions of f_{max} were used: frequency at which spectral power decreases down to 0.1 of its maximum value, modified threshold crossing method [23] and novel geometrical method. "Goodness" and efficiency of estimators were determined calculating the bias and standard deviation of the estimated mean and maximum frequency of the computer simulated Doppler spectra. The power of analysed signals was assumed to have the exponential distribution function. The SNR ratios were changed over the range from 0 to 20 dB. The AR and ARMA models orders selections were done independently according to Akaike Information Criterion (AIC) and Singular Value Decomposition (SVD). It was found, that the ARMA model computed according to SVD criterion had the best overall performance and produced the results with the smallest bias and standard deviation. The preliminary studies of the AFT proved its attractiveness in real-time computation, but its statistical properties were worse than that of the other estimators. It was noticed that with noise subtraction the bias of f_{mean} decreased for all tested methods. The geometrical method of f_{max} estimation was found to be more accurate of other tested methods, especially for narrow band signals.

1. Introduction

Doppler ultrasound is widely used technique for measuring of blood flow in vessels. The proper estimation of mean and maximum Doppler frequency is crucial for flow quantification. The mean Doppler frequency (f_{mean}) carries the information on the mean blood flow velocity; for known vessel diameter, the volumetric flow can be then computed. The detection of the maximum frequency (f_{max}) is a good indicator of narrowing of the vessel. The tighter the stenosis is, the higher is the expected velocity.

Different methods of the estimation of the Doppler frequencies in the time and frequency domains are described in literature [4, 17, 25, 28]. The performance of both parametric and non-parametric spectral estimators was done by VAITKUS et al. [38], but there is however, a lack of analysis of assessment of the influence of the applied spectral estimation methods on maximum Doppler frequency measurement.

The influence of four methods used for modelling of the power spectral density (PSD) on mean and maximum frequency estimation is described in this paper. The examined methods were: FFT, AR Burg, ARMA and arithmetic Fourier transform (AFT). For all mentioned spectrum estimators the mean frequency was computed as the first moment of the spectrum with and without noise subtraction. The novel geometrical method of f_{max} determination is described and compared with other methods described by d'ALESSIO [12] and Mo et al. [23]. The evaluation was done using computer simulated stationary Doppler signals with added white noise.

Performance of examined estimators was determined by calculating bias and standard deviation of f_{mean} and f_{max}.

2. Doppler signal modelling

The early theoretical and experimental work of SHUNG et al. [30] showed that the scattering of ultrasound in blood was proportional to the fourth power of frequency.

The scattering was found to depend upon the hematocrit HTC of blood. The increase of scattering was observed for HTC up to 24% reaching the plateau between 24% and 30% and next decrease occured. SHUNG et al. [30] concluded that for HTC greater than 20% the assumption of the independent backscattering was rather unrealistic. Their results were in good agreement with TWERSKY's [36] wave scattering theory for small scatteres and heuristic "hole" approach [30].

A number of works on multiple scattering of acoustic waves in media with a small fractional volume were published [15]. The higher order approximation [21] for higher fractional volume of scatterers resulted in better understanding of scattering phenomena. Another approach was presented by ANGELSEN [3] assuming that the backscattered signal originated from the variations of the local density and compressibility of blood.

However, the existing theoretical descriptions are not complete to incorporate the effect of multiple scattering for the ultrasonic field parameters. For this reason we have neglected in this work multiple scattering and the effect of the interaction between the red cells in blood. The applied model is similar to the one used by ATKINSON and WOODCOCK [5], FERRARA [14] and HOLLAND [16]. We have neglected such factors as beam sensitivity and attenuation in the tissue.

Let the transmitted signal be of the form

$$s(t) = A\cos(\omega_0 t), \tag{1}$$

where ω_0 is the radial transmitted frequency.

The ultrasonic signal backscattered from the population of the red cells can be approximated by

$$f(t) = \sum_i A_i \cos(\omega_i t + \varphi_i), \tag{2}$$

where A_i and φ_i are respectively amplitudes and phases of the echo backscattered at i-th scatterer.

Since the backscattered Doppler echo is a single-sideband like signal (with suppressed carrier) it is convenient to represent it by analytical signal $Z(t)$ derived from the real function $f(t)$ using the Hilbert transform $F_H(t)$.

Function $F_H(t)$ is a quadrature function of $f(t)$ because all of their frequency components are shifted by $\Pi/2$ with respect to $f(t)$.

In polar coordinates $Z(t)$ can be written as

$$Z(t) = |Z(t)|\, e^{\omega_i t + \varphi_i},$$

where

$$|Z(t)| = \sqrt{f^2(t) + F_H^2(t)}, \qquad \omega_i t + \varphi_i = \arctan\left(\frac{F_H(t)}{f(t)}\right). \tag{3}$$

The amplitude of analytical signal determines its instantaneous amplitude or envelope while time rate of change of its phase is the instantaneous frequency.

Quadrature components $f(t)$ and $F_H(t)$ are the real and imaginary parts of the input signal. The frequency of input signal is increased or decreased by a value of Doppler shift ω_d originated at moving particles.

After mixing $Z(t)$ with reference signals $\sin(\omega_0 t)$ in one channel and $\cos(\omega_0 t)$ in second channel two base band quadrature signals are obtained

$$\begin{aligned} I(t) &= f(t)\cos(\omega_0 t) + jF_H(t)\sin(\omega_0 t) \\ Q(t) &= -f(t)\sin(\omega_0 t) + jF_H(t)\cos(\omega_0 t) \end{aligned} \tag{4}$$

Since the position of blood particles is random, $I(t)$ and $Q(t)$ components of the backscattered signal are random variables. Each particle is an independent source of echo with random phase φ_i, Doppler phase $\omega_i t$ and amplitude A_i.

For stationary targets the random phase is equal to

$$\varphi_i = \frac{4\pi d_i}{\lambda}, \tag{5}$$

where d_i is the distance from the transducer to the i-th scatterer and λ is the wavelength, $\lambda = c/f_0$, c is the speed of sound in blood.

When particles are moving with radial velocity v_{ri} towards (or away) the transducer then the rate of change of phase, called the Doppler shift, is equal to

$$\frac{d\varphi_i}{dt} = \frac{4\pi v_{ri}}{\lambda} = \omega_{di}. \tag{6}$$

Both stationary random phase and Doppler phase can be combined together. After replacing φ_i in Eq. (2) by $\varphi_i + \omega_{di} t$. the demodulated analytical signal $Z_d(t)$ becomes

$$Z_d(t) = \sum_i A_i \cos(\omega_{di} t + \varphi_i) + j \sum_i A_i \sin(\omega_{di} t + \varphi_i). \tag{7}$$

The insonified field or sample volume is much larger than the wavelength ($ct >> \lambda$). For large number of scatterers in the sample volume, the probability distribution of φ_i is expected to have uniform density function within the range $-\Pi$, $+\Pi$. In fact, between the minimum and maximum values of d_i, φ_i spans over many intervals of 2Π, folding into the $-\Pi$ and $+\Pi$ range, justifying even better the assumption of uniform distribution.

The central limit theorem states that the distribution of sufficiently large sum of independent random variables approaches a Gaussian distribution.

Applying this theorem to the Eq. (7) we can conclude that both real $I(t)$ and imaginary $Q(t)$ components of complex envelope $Z(t)$ are independent random variables and have Gaussian distribution with zero mean. It yields that the distribution of amplitude A of complex envelope is equal to the joint probability distribution of $I(t)$ and $Q(t)$

$$p[I(t), Q(t)] = p[I(t)]\,p[Q(t)] = \frac{1}{2\pi\sigma^2}\, e^{-\frac{(I^2(t)+Q^2(t))}{2\sigma^2}}, \tag{8}$$

Replacing the variables $I(t)$ and $Q(t)$ by their equivalents in the polar coordinates, $A = \sqrt{(I^2+Q^2)}$ and $\varphi = \arctan(I/A)$, the joint density function becomes

$$p[A,\varphi] = \frac{A}{2\pi\sigma}\, e^{-\frac{A^2}{2\sigma^2}}, \tag{9}$$

The distribution of φ_i alone is uniform and equal to $1/(2\Pi)$ over $\langle -\Pi..\Pi\rangle$.

The distribution of A alone is given by

$$p[A] = \frac{A}{\sigma^2}\, e^{-\frac{A^2}{2\sigma^2}} \tag{10}$$

for $A>0$.

The simulated Doppler signal should have the statistical properties identical or at least similar to that of the backscattered ultrasonic signal from the blood. The time averaged spectral density of C.W. Doppler (continuous wave Doppler) signal for parabolic blood velocity profile is uniform within the range from $f_{\min}$ up to $f_{\max}$ corresponding to the minimum and maximum velocity of blood [7]. For pulse Doppler, the backscattered energy returns from a small sample volume and the time averaged spectrum is considerably narrowed. Also for C.W. Doppler, combination of narrow ultrasonic beam and flat blood velocity profile result in narrow Doppler spectrum. Without introducing a substantial error the envelopes of those spectra can be approximated by the Gaussian functions. The similar approach was used in modelling of radar precipitation signals [13, 31].

The resulting spectral envelope becomes

$$G_n = \frac{1}{\sigma\sqrt{2\pi}}\, e^{-\frac{(f_n-\mu)^2}{2\sigma^2}}, \tag{11}$$

where G_n is the discrete spectral coefficient at frequency f_n, μ is a power weighted mean frequency and σ is the standard deviation of the spectrum.

This approach facilitates control over the simulated mean frequency and the bandwith 2σ of the Doppler spectrum.

The noise present in the Doppler signal is assumed to be a white one. The amplitude of the backscattered ultrasound has Rayleigh distribution (see Eq. (10)). It was shown [31, 32] that the amplitude of sum of the signal and noise must have Rayleigh distribution function and its power P_n must be exponentialy distributed

$$p[P_n] = \frac{1}{\sigma_s^2} e^{-\frac{P_n}{\sigma_s^2}}, \tag{12}$$

where σ_s^2 equals to the average power of the signal.

The generation of random variable having a particular distribution is accomplished using an inverse cumulative distribution function (CDF) transformation [22, 26]. If a source of uniformly distributed random variables x_n is presupposed then a random variable P_n are obtained according to

$$P_n = \sigma_s^2 \ln(x_n). \tag{13}$$

The proper scaling of signal and noise depends on SNR value defined as

$$\mathrm{SNR} = 10 \log_{10} \left(\frac{\sum_n G_n}{\sigma_{ns}^2} \right), \tag{14}$$

where ΣG_n is the power of the signal and σ_{ns}^2 is noise power.

Now, we may replace average power σ_s^2 in (13) by an expression including the spectral envelope G_n and SNR [31].

$$\sigma_s^2 = \frac{\sigma_{ns}^2 10^{\frac{\mathrm{SNR}}{10}}}{\sum_n G_n} G_n + \frac{\sigma_{ns}^2}{N} \tag{15}$$

and finally we arrive at the expression describing the composite spectral density outlined by Gaussian envelope G_n

$$P_n = \left(\frac{\sigma_{ns}^2 10^{\frac{\mathrm{SNR}}{10}}}{\sum_n G_n} G_n + \frac{\sigma_{ns}^2}{N} \right) \ln(x_n), \tag{16}$$

The next step is to obtain the real A_n and imaginary B_n components of the composite spectrum. The amplitudes of real part A_n and imaginary part B_n of the composite spectrum are Gaussian distributed

$$A_n = \sqrt{P_n}\cos(2\pi x_n)$$
$$B_n = \sqrt{P_n}\sin(2\pi x_n). \tag{17}$$

The properties of CDF transformation were applied here again; the products of Rayleigh distributed $\sqrt{P_n}$ and cos $(2\Pi x_n)$ or sin $(2\Pi x_n)$ where x_n is uniformly distributed over the range {0,1}, generate two independent Gaussian distributed processes.

Finally, the quadrature time signals are obtained by inverse Fourier transform of the composite spectrum

$$\mathcal{F}^1\{A_n + jB_n\} = I(t) + jQ(t). \tag{18}$$

The variable parameters of simulated Doppler spectra were: mean frequency, maximum frequency, bandwith and signal to noise ratio SNR, varied from 0 to 20 dB (0, 3, 6, 10, 20 dB). The sampling rate was set to 20 kHz. The signal was generated according to (17) using a 1024 points FFT, and only the real part of the signal was considered in further analysis. Every realization of such random processes was simulated by a block of 3072 adjacent samples. Those time series were observed using a 128 pts. Hamming window in order to achieve local stationarity of the signal and to reduce Gibbs phenomena.

The mean frequency of the Gaussian enveloped spectrum was changed from 1250 Hz to 7000 Hz. Different spectra widths were controlled by setting standard deviation σ (Eq. (14)) equal to 16, 32 and 64 points or, in frequency units, 320 Hz, 640 Hz and 1280 Hz.

Along with the Gaussian enveloped spectra the rectangular spectra of 320 Hz and 1280 Hz bandwidth were generated in order to simulate the parabolic flow insonified uniformly by C.W. Doppler.

3. Estimation of PSD

3.1. Periodogram

The periodogram was chosen as the reference method. The power spectral density function (PSD) was estimated as:

$$P_{\mathrm{PER}}(f) = \frac{1}{N}\left|\sum_{n=0}^{N-1} x(n)\, e^{-j2\Pi f n}\right|^2. \tag{19}$$

In spite of well known advantages of the periodogram (known statistics, medium computational cost, good performance for noisy signals), this PSD estimator performance suffers from both an increased variance (regardless of the observation time window), as well as spectral leakage due to the implicit windowing of the data. In analysis of the Doppler signals it causes an unreliable f_{mean} and f_{max} estimation for low SNRs. Reduction of the estimator's variance, through averaging of succeeding or

overlapping data segments is one of the remedy, however limited for real-time signal processing.

3.2. Periodogram via Arithmetic Fourier Transform (AFT)

REED et al. [27] proposed an algorithm of Fourier coefficients determination with linear computational cost (only one multiplication per Fourier coefficient with number of addition comparable to FFT). This very efficient method is based on inverse Mobius theorem. According to this theorem, every function $f(n)$, not vanishing in $<1, N>$ and vanishing outside $<1,N>$ ($f(n) = 0$, for $n>N$) may be expressed as

$$f(n) = \sum_{m=1}^{\text{trunc}(N/n)} \mu(m)\, g(mn), \tag{20}$$

where

$$g(n) = \sum_{k=1}^{\text{trunc}(N/n)} f(kn).$$

with $\mu(m)$ denoting Mobius function and trunc(x) denoting integer part of real number x.

Then the real continuous signal $A(t)$ with zero mean, has n-th average shifted by α defined as

$$S(n,\alpha) = \frac{1}{n} \sum_{m=0}^{N-1} A\left(\frac{mT}{n} + \alpha T\right). \tag{21}$$

The real and imaginary parts of Fourier coefficients may be expressed as

$$\text{RE}\{F_n\} = \frac{c_n(0)}{2} \qquad \text{for } n=1...N \tag{22}$$

and

$$\text{IM}\{F_n\} = -\frac{(-1)^m c_n\left(\frac{1}{2^{k+2}}\right)}{2}, \quad \text{for } k=0,...,\text{trunc}(\log_2 N)-2,\ n=2^k(2m+1), \tag{23}$$

where

$$c_n(\alpha) = \sum_{i=1}^{\text{trunc}(N/n)} \mu(l)\, S(\ln,\alpha). \tag{24}$$

The summation in (21) is performed for continuous indices, so in the case of sampled signals the interpolation of values for time instants between samples is necessary. As it was shown in [35], in order to get N spectral coefficients a set of D_N samples is needed

$$D_N = 3\left(\frac{N}{\Pi}\right)^2 + O(N \ln N). \tag{25}$$

For example, over 1500 samples of time signal should be taken to obtain exact 64 complex Fourier coefficients. This rather large number of samples can be reduced by interpolation of analyzed signal, although it creates some distortion of the results.

The interpolation may be done simply by taking nearest neighbouring samples, i.e. zero-order interpolation. For 128-points segment of a sinusoidal signal the maximum error caused by zero-order interpolation is less than 1%. For realization of random Gaussian process the mean square error depends on autocorrelation function (ACF) and number of coefficients [27]. For signals with Gaussian envelope those errors vary from 0.013 to 0.201 of signal power depending on signal bandwidth. For linear interpolation those errors are neglible, but the computing time increases considerably.

The AFT method is well suited for real-time application, especially in parallel structures.

3.3. *Autoregressive modelling* (AR)

The PSD of an autoregressive model of analysed signals (PSD-AR) was calculated according to

$$P_{\mathrm{AR}}(f) = \frac{s^2}{\left|1 + \sum_{k=1}^{p} a(k)\, e^{-j2\Pi fk}\right|^2} \tag{26}$$

where $a(k)$ are model coefficients, p — model order and s^2 — total squared error of the model.

The spectral envelope of the AR model is smooth. This estimator is asymptotically unbiased and for large n (and $N > 2p$) its variance is smaller than for the periodogram [19].

The accuracy of such PSD estimation is limited, due to the limited ability of proper modelling of time series as the autoregressive process. Thus, the PSD-AR of the signal with wideband Gaussian spectral envelope will be biased, also the PSD of noisy signal will be distorted. For narrowband process with a Gaussian spectral envelope the bias is small. In spite of these, AR modelling is widely used in analysis of Doppler signals [18, 37], primary merited by its excellent resolution and good spectral match. It should be noted however, that for low SNR the resolution of the AR spectral estimator is no better than that of the periodogram. Kay [20] concluded, that the effect of injected white noise is to produce a flattened PSD-AR estimate, regardless of the nature of the observed process. In our modelling scheme we have found however, that for Doppler signals (with Gaussian spectral envelope) the prediction error was proportional to SNR, if the model order was optimal (PSD-AR close to true PSD).

We have tested two model identification procedures. First, the model order was determined due to the Akaike Information Criterion (AIC) [2]

$$\mathrm{AIC}(p) = N \ln s + 2p \tag{27}$$

The common method of autoregressive coefficients determination is to estimate autocorelation lags of considered signal and then to solve a set of linear equations called Yule-Walker equations (YWE) [20]. Since the solution of the YWE introduces the smallest amount of peaking in the spectrum of the 'colored noise' [19], therefore we postulate the use of YWE for model order identification of the Doppler signals.

The Singular Value Decomposition (SVD) of the overdetemined YWE (primary selection of model order is greater than expected) may be used for construction of the normalized matrix approximation ratio [11]

$$\upsilon(k) = \frac{\| \mathbf{R}^{(k)} \|}{\| \mathbf{R} \|} = \sqrt{\left(\frac{\sigma_1^2 + \sigma_2^2 + \ldots + \sigma_k^2}{\sigma_1^2 + \sigma_2^2 + \ldots + \sigma_r^2} \right)} \tag{28}$$

where $\mathbf{R}$ — autocorrelation matrix with rank r, $\mathbf{R}^{(k)}$ — submatrix with rank k and σ_i — singular values of $\mathbf{R}$. The ratio $\upsilon(k)$ approaches 1, if k equations completely describes AR model of signal, e.g. for signals without noise. For noisy signals, the construction of overdetermined YWE is rather impossible and the ratio $\upsilon(k)$ doesn't reach unity till $r=k$. CADZOW [11] proved however, that for $\upsilon(k)$ close to unity, $\mathbf{R}^{(k)}$ is the best approximation of $\mathbf{R}$ in the least square sense. Consequently, the selection of the model order was done observing the progression of $\upsilon(k)$ with increasing k. The value of k for which the ratio $\upsilon(k)$ was reaching "plateau" (typically for $\upsilon(k)$ equal to 0.999) was chosen as the AR model order.

Usually, the model order described by SVD was greater than the one obtained by AIC and was used here for model identification only. The difference was observed especially for signals with low SNR and larger bandwidth.

3.4. ARMA *modelling*

The signal described as concatenation of AR and MA processes has the PSD expressed as

$$P_{\mathrm{ARMA}}(f) = \left| \frac{\sum_{k=0}^{q} b(k) e^{-j2\Pi f k}}{\sum_{k=1}^{p} a(k) e^{-j2\Pi f k}} \right|. \tag{29}$$

The ARMA model often provides better spectral estimates than either AR or MA models. Simultaneous evaluation of both a and b parameters in Eq. (29) is computationally ineffective, so the suboptimal solutions should be rather used. We applied the least square solution, based on the CADZOW's [10] least square method (LSMYWE) to tune between better statistical properties and computational cost [20]. The MA coefficients were computed according to Durbin's method [19].

The theroretical considerations concerning variance of the estimator [33] leads to the conclusion, that LSMYWE give asymptotically unbiased estimator with variance monotonically decreasing with increasing number of equations ($N>>p$).

Although numerous techniques were developed, the common solution is to estimate the order of AR process and next to select $q=p$ in (29). This is based on observation of small sensivity of overall ARMA model to inaccuracies in MA identification[1]. The SVD method (applied to the modified YWE) was used for determination of the number of poles p and next the order of MA process was assumed to be equal to the AR order.

4. Mean frequency estimation

The mean frequency was estimated as a first spectral moment of the simulated signal (F1 method):

$$Kv_{\text{mean}} = f_{\text{mean}} = \frac{\int_0^{f_{\max}} fP(f)\,df}{\int_0^{f_{\max}} P(f)\,df} = \frac{\sum_i f_i P(f_i)}{\sum_i P(f_i)}. \tag{30}$$

Since Eq. (30) estimates the mean of the composite Doppler signal plus noise, so it includes additional bias due to the noise.

One of the simplest method of noise suppression is to subtract the noise spectral density ($N(f)$) from the derived spectrum and then to calculate the mean (F1-NS method):

$$f_{\text{mean(NS)}} = \frac{\sum_{i=0}^{N-1} f_i(P(f_i)-N(f_i))}{\sum_{i=0}^{n-1} (P(f_i)-N(f_i))}. \tag{31}$$

The noise spectral density $N(f)$ was estimated from the tail of the spectrum, beyond maximum frequency od Doppler signal. SIRMANS and BUMGARNER [31] concluded, that the F1-NS method provided the unbiased estimation of f_{mean} even for low SNRs and that the standard deviation of this estimator was small.

In our study, both, first moment (F1) and first moment with noise suppression (F1-NS) methods were used for mean frequency estimation of all spectral estimators.

5. Maximum frequency estimation

The estimation of $f_{\max}$ is a rather complicated task, resulting from the random nature of Doppler signal and the presence of noise. The misrepresention may occur during the observation of low-level signal in noisy environment.

Since the PSD of the random signal with Gaussian spectral envelope is unbounded, so $f_{\max}$ was defined as the frequency at which spectral power decreased down to 0.1 of its

[1] The pure MA model was rejected after primary analysis due to its poor performance.

maximum value (method 0.1max), although it was realiable only for smoothed PSD (AR, ARMA).

Along with 0.1max two other f_{max} estimators — d'Alessio percentile and modified threshold crossing (MTCM) [23] were examined. It was confirmed, that their behavior strongly depend on SNR, noise level N(f) and the shape of time windowind functoin of the analysed signal.

The novel geometrical method is simpler, being sufficiently precise and computational effective. The integrated power spectrum [23] is equal to

$$\Phi(f) = \int_{f_l}^{f} P(f)\, df. \tag{32}$$

The basic idea of our method is as follows. First the power spectral integral $\Phi(f)$ is computed. Next the straight line connecting two points on $\Phi(f)$ corresponding: 1. to the maximum analysed frequency ($\Phi(f_h)$) and 2. to the value of f_{mode} for which the peak spectral power is maximum ($\Phi(f_{mode})$) is constructed. Then the distance from this line to $\Phi(f)$ is computed for all frequencies greater than f_{mode}. Finally, the frequency at which the distance is maximum is assumed to be the maximum frequency of the signal. On the Fig. 3 an example of $\Phi(f)$ is presented; f_{mode} denotes the frequency where P(f) reaches maximum value, f_h is maximum analysed frequency.

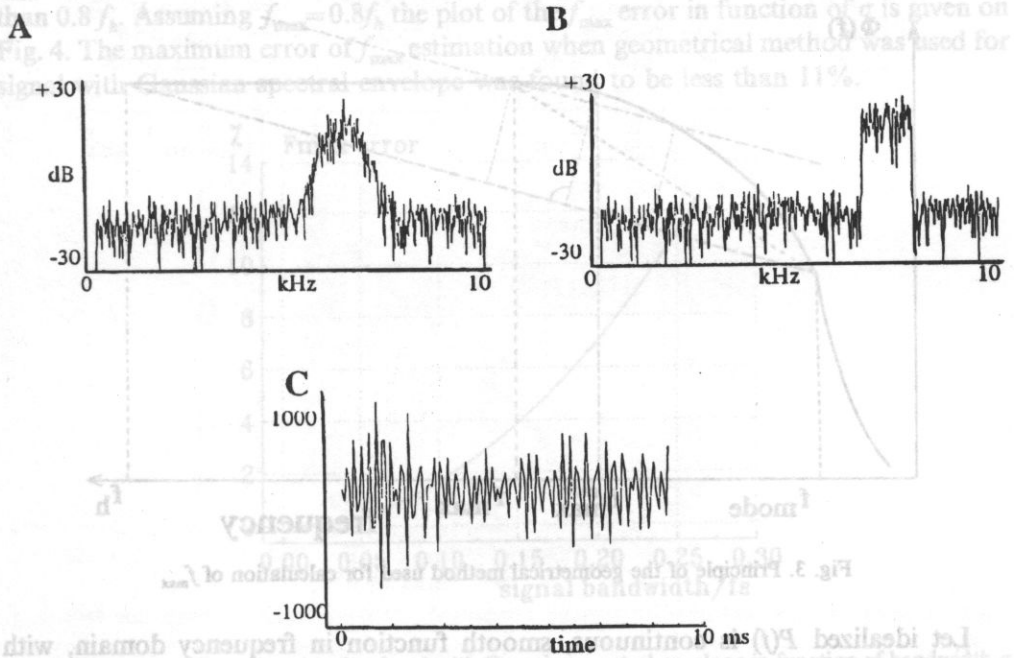

Fig. 1. Simulated spectra, SNR = 20 dB; a) Gaussian envelope, b) rectangular envelope, c) time signal for Gaussian envelope.

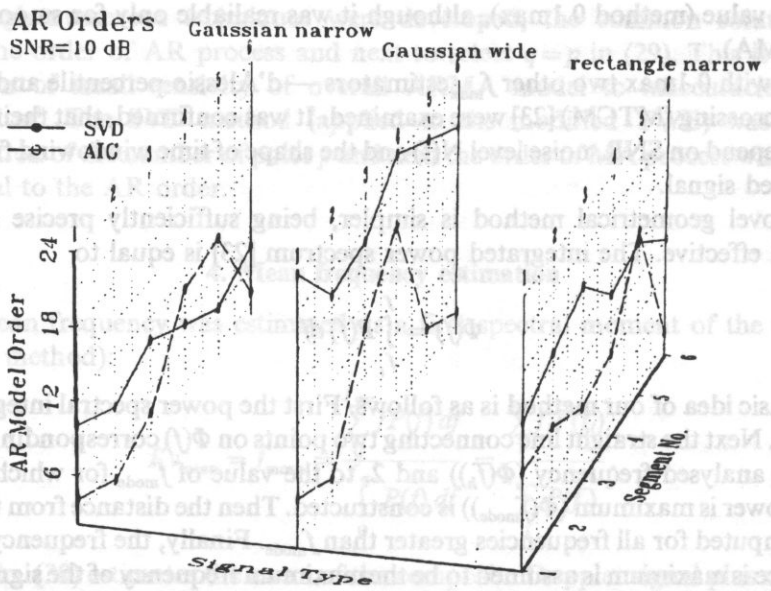

Fig. 2. Examples of AR models orders obtained by AIC and SVD for realizations of the identical processes a) narrow band Gaussian envelope, b) wide band Gaussian envelope, c) rectangular spectrum.

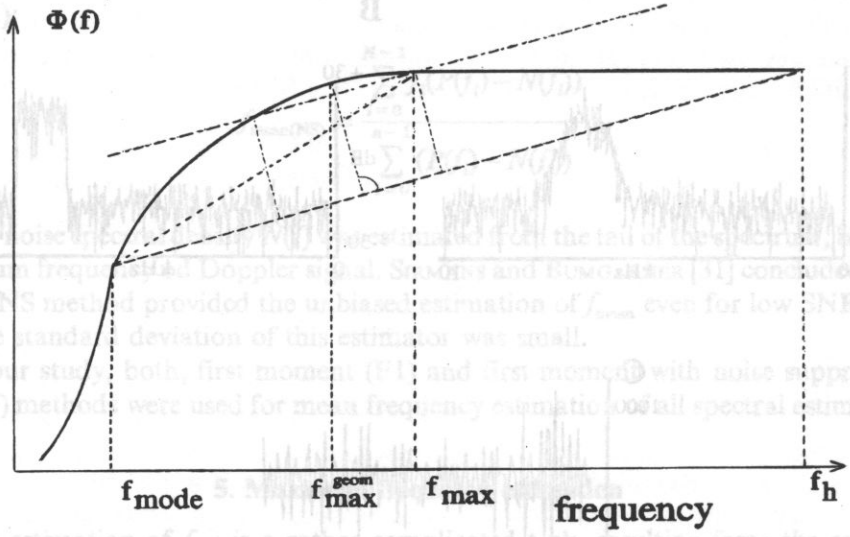

Fig. 3. Principle of the geometrical method used for calculation of f_{max}

Let idealized $P(f)$ is continuous, smooth function in frequency domain, with a single maximum for f_{mode}. Assuming that no noise is present, $P(f)=0$, for $f>f_{max}$.[2] Let

[2] For averaged spectrum, we can assume that additional noise causes rotation of $\Phi(f)$ relative to axes over the arc of arctan $(N(f))$ radian.

$\Phi(f)$ denotes integral of $P(f)$ according to (32). Then, begining at f_{max} $\Phi(f)$ becomes parallel to f axis and the slope α of the straight line $\Phi(f_{mode})$ $\Phi(f_h)$ is equal to

$$\alpha = \frac{\Phi(f_h) - \Phi(f_{mode})}{f_h - f_{mode}}. \tag{33}$$

The distance d is maximum for $f \in <f_{max}, f_n>$ and such estimation of f_{max} has no positive bias. For frequencies within $<f_{mode}, f_{max}>$ the error of the method depends on proportions between slope of $\Phi(f)$ and slope of the $\Phi(f_{mode})$ $\Phi(f_h)$ line. $D(f)$ is maximum at point $f=f_{max}$ if, and only, if the slope of the line $\Phi(f)\Phi(f_{max})$ is greater then the slope of the line $\Phi(f_{mode})\Phi(f_h)$

$$\forall (f_{mode} \leqslant f \leqslant f_{max}) \quad \frac{\Phi(f_h) - \Phi(f_{mode})}{f_h - f_{mode}} > \frac{\Phi(f_{max}) - \Phi(f)}{f_{max} - f}. \tag{34}$$

According to (34): 1. the error is maximum, when $f_{max}=f_h$, 2. the underestimation of f_{max} is decreasing, when $P(f)$ is slowly decreasing for increasing frequency.

Let consider the case of the signal with a Gaussian spectral envelope (Eq. (11)). Its maximum frequency was defined as the frequency at which the spectral envelope decreased to 0.1 of its maximum value. For Gaussian spectral envelope $f_{max} \approx f_{mode} + 2.1\sigma$. Practically, the examined Doppler signals extended only to f_{max} less than $0.8 f_h$. Assuming $f_{max}=0.8 f_h$ the plot of the f_{max} error in function of σ is given on Fig. 4. The maximum error of f_{max} estimation when geometrical method was used for signal with Gaussian spectral envelope was found to be less than 11%.

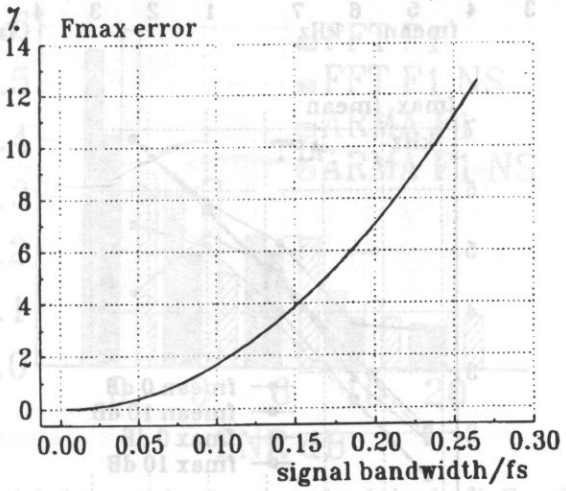

Fig. 4. The error of f_{max} estimation for signal with Gaussian spectral envelope in function of bandwidth σ.

According to Eq. (34) the maximum frequency of signals with rectangular spectral envelope was estimated with no errors.

6. Results and discussion

FFT, AFT, AR Burg and ARMA were tested for PSD estimation of all simulated random processes. F_{mean} was computed using PSD's first moment with and without noise substraction. Finally, f_{max} was computed using 0.1 max method, d'Alessio, threshold crossing method and novel geometrical method. The results were compared to the reference f_{max} selected during simulation at the level of 10% of the peak spectral power. The bias and standard deviation of estimators were computed and compared for every data file (24 data blocks of 128 samples length) for varying SNR (0, 3, 6, 10, 20 dB).

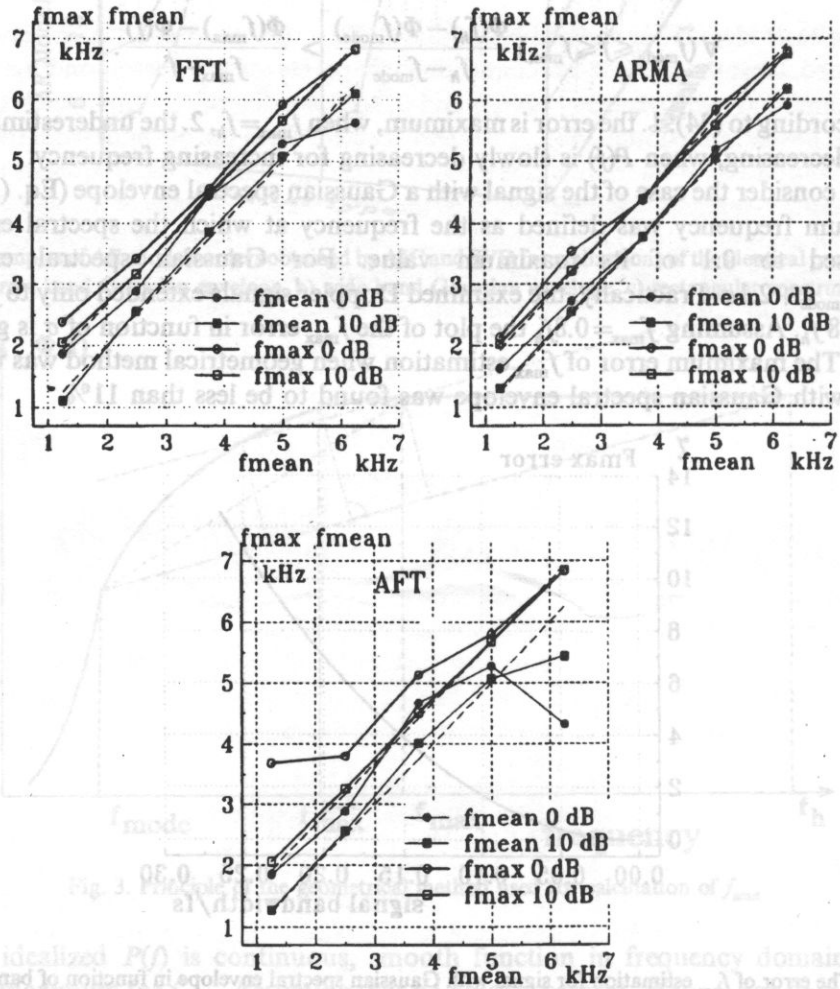

Fig. 5. F_{mean} and f_{max} in function of true f_{mean} for narrow band Gaussian spectrum signal; a) FFT b) ARMA c) AFT for different SNRs (0 dB and 10 dB).

The comparison of different PSD estimations for signal with a narrow-band Gaussian spectral envelope is presented on Fig. 5.

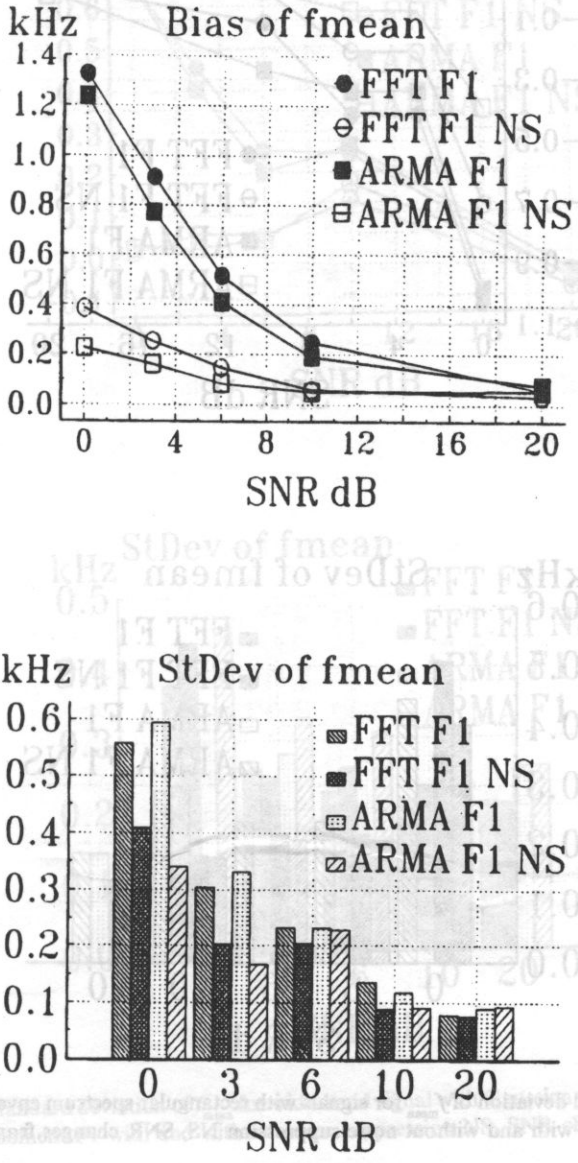

Fig. 6. Bias and standard deviation of f_{mean} for narrow band signal with Gaussian spectrum envelope computed using first moment F1 with and without noise suppression NS, SNR changes from 0 to 20 dB.

The bias of the mean frequency estimation for variable SNRs was lower for the F1-NS method than for F1 method. The standard deviation remained almost unchanged for both, FFT and ARMA methods, (Fig. 6, 7 and 8).

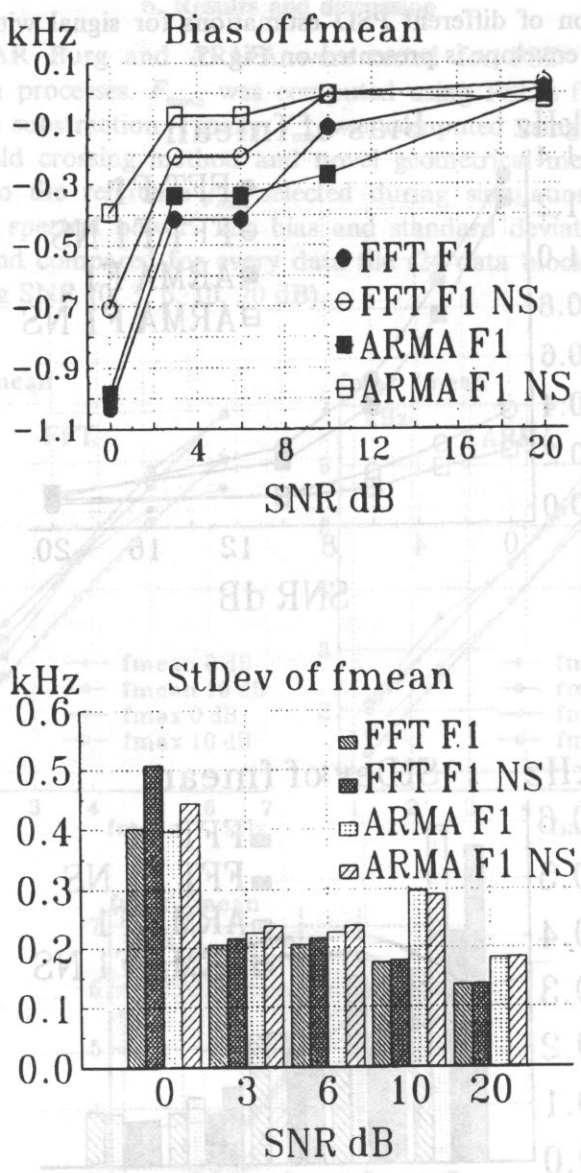

Fig. 7. Bias and standard deviation of f_{mean} for signals with rectangular spectrum envelope computed using first moment F1 with and without noise suppression NS, SNR changes from 0 to 20 dB.

The comparison of f_{max} estimators proved the advantages of the geometrical approach (Fig. 9, 10 and 11) over other tested methods. The bias was significantly reduced, especially for very low SNR's. A reduction in standard deviation was observed showing a significant improvement in performance. Considering the PSD estimation, ARMA modelling was found superior for f_{mean} and f_{max} estimation, while

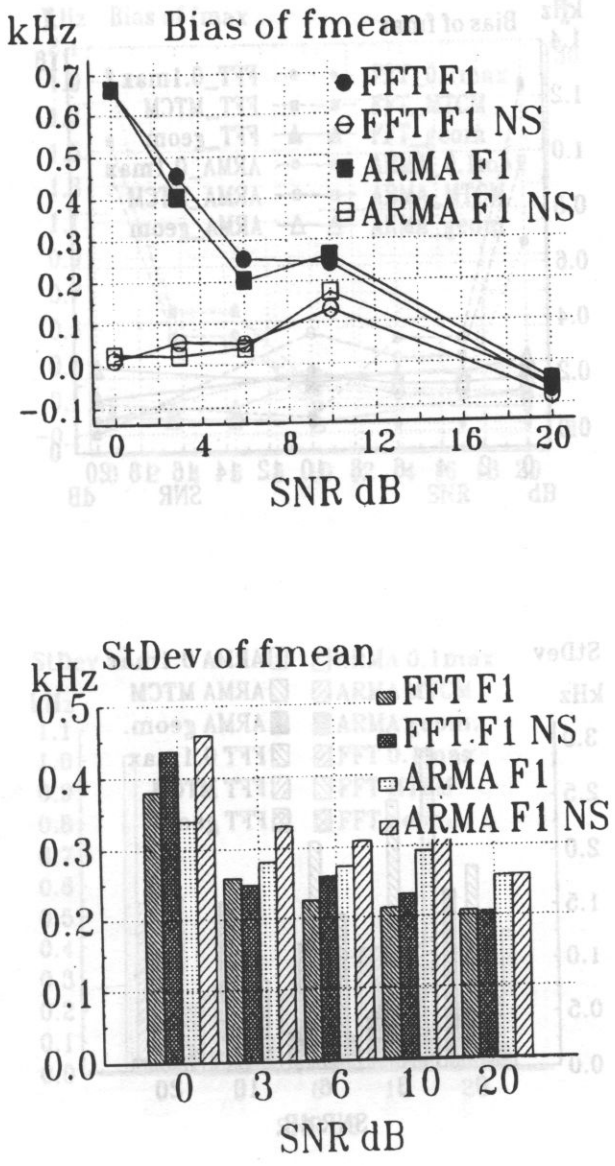

Fig. 8. Bias and standard deviation of f_{mean} for wide-band signal with Gaussian envelope spectrum computed using first moment F1 with and without noise suppression NS, SNR changes from 0 to 20 dB.

the AFT method was apparent worse, especially for low SNR's. The AR model of PSD with order selection after Akaike criterion was found to produce the mean frequency estimation comparable to the one achieved with AR model when order selection was calculated using SVD. The SVD AR performed better for f_{max} estimation.

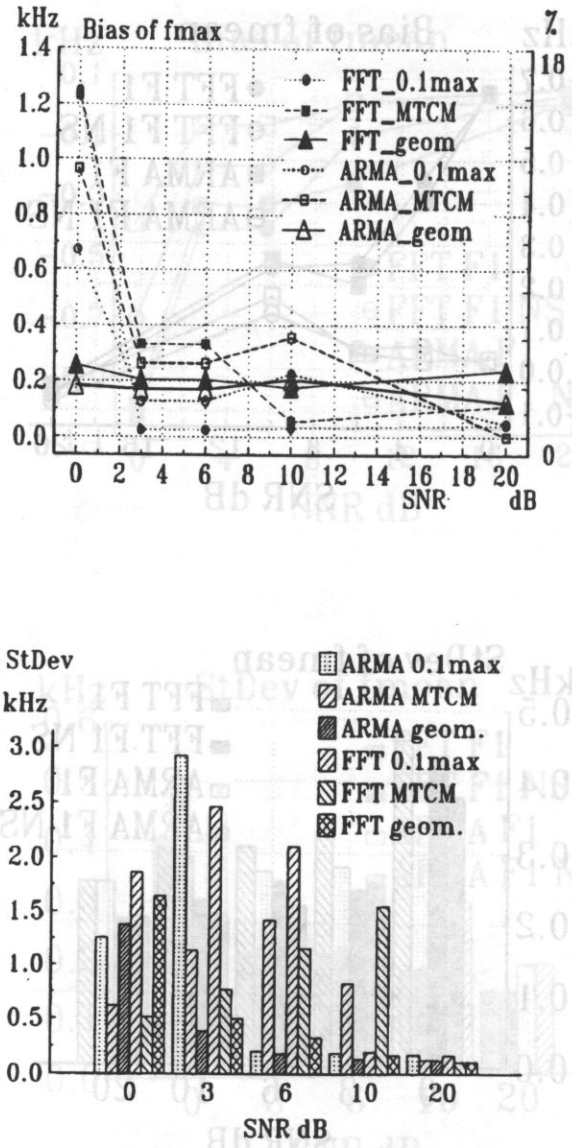

Fig. 9. Bias and standard deviation of f_{max} for narrow band signal with Gaussian envelope spectrum computed using 0.1max, MTCM and geometrical methods, SNR changes from 0 to 20 dB.

The overall performances of both: PSD estimation methods and f_{mean} and f_{max} computations, proved to be similar also for signals with medium and wide band Gaussian envelope, although the bias and standard deviation grew with growing signal bandwidth.

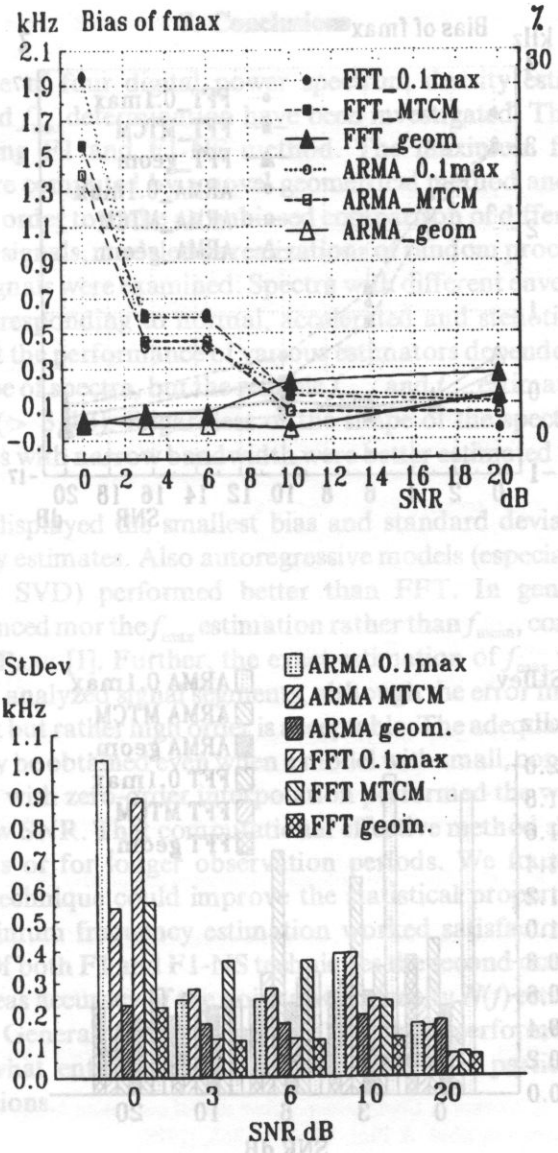

Fig. 10. Bias and standard deviation of f_{max} for signals wigh rectangular spectrum envelope computed using 0.1max, MTCM and geometrical methods, SNR changes from 0 to 20 dB.

For rectangular spectra the differences between the efficiency of estimation of f_{mean} and f_{max} were smaller than for signals with a Gaussian spectral envelope due to more distinct modelling of examined quantities (Fig. 10). The PSDs evaluation has given no unique differences for all methods except AFT. F_{mean} was still better approximated by F1-NS method. The smallest bias and standard deviation of f_{max} were found using the

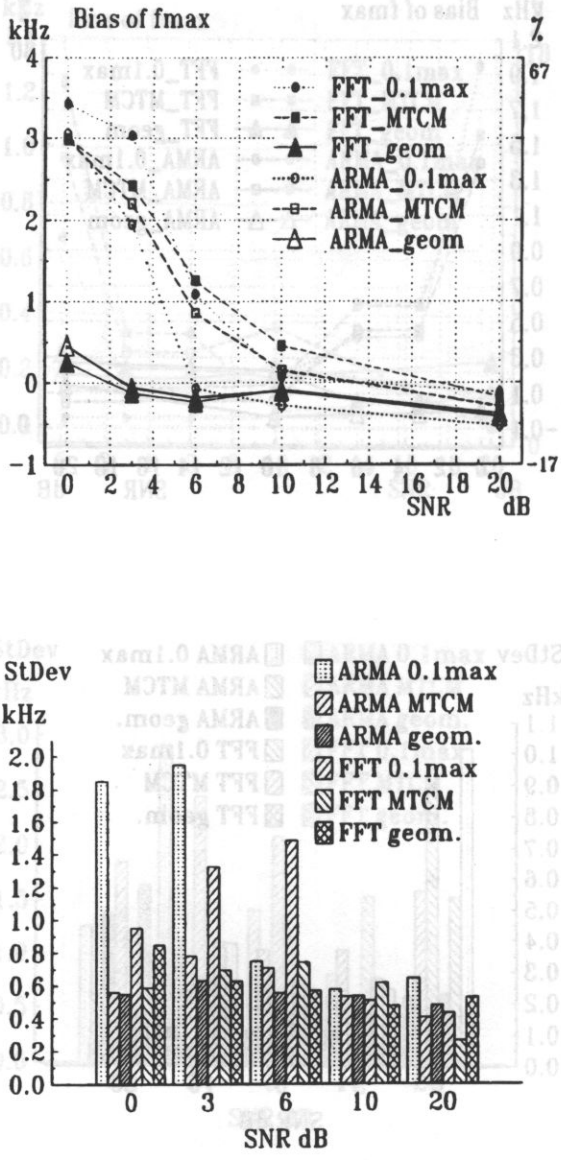

Fig. 11. Bias and standard deviation of f_{max} for the signals with wide-band Gaussian spectrum envelope computed using 0.1max, MTCM and geometrical methods, SNR changes from 0 to 20 dB.

geometrical method. From all other methods of f_{max} estimation the MTCM performed the best, but was comparable to geometrical one only for SNRs > 6 dB. The location of f_{mode} didn't affect the results. Generally, the bias and standard deviation of the results were increasing for wider spectra (Fig. 9 and 11).

7. Conclusions

The performance of four digital power spectrum density estimators and their influence on f_{mean} and f_{max} determination have been investigated. The mean frequency was determined using F1 and F1-NS method. The maximum frequencies of the Doppler spectra were computed by a novel geometrical method and compared to the other techniques. In order to make an unbiased comparison of different estimators the computer simulated signals, modeled as realizations of random processes equivalent to real Doppler flow signals were examined. Spectra with different envelopes were used to simulate signals corresponding to normal, accelerated and stenotic blood flows.

It was found that the performance of various estimators depended on SNRs, signal bandwidth and shape of spectra, but the reliable f_{mean} and f_{max} estimation were obtained also for low SNRs ($>$ 3 dB). Regardless of the shape of the spectrum and the PSD estimator, the signals with narrow bandwidth were better estimated than the wideband signals.

ARMA model displayed the smallest bias and standard deviation of mean and maximum frequency estimates. Also autoregressive models (especially with the model order predicted by SVD) performed better than FFT. In general, exact model identification influenced mor the f_{max} estimation rather than f_{mean}, confirming the recent results of AHN and PARK [1]. Further, the exact estimation of f_{max} needs model order identification for all analyzed signal segments, although the error introduced using the model with constant but rather high order is acceptable. The adequate estimation of the mean frequency may be obtained even when a model with small, constant order is used.

AFT estimation with zero-order interpolation performed the worse, especially for signals with very low SNR. That computational effective method should be used only for "strong" signals or for longer observation periods. We found, that the use of "sliding window" technique could improve the statistical properties of AFT.

Mean and maximum frequency estimation worked satisfactory only for signals with SNR $>$ 3 dB. Of both F1 and F1-NS techniques the second one was giving usually better results, whereas accuracy of the noise power density $N(f)$ estimation was limited [Mo et al., 1988]. Generally, the geometrical method performed the best for all analyzed signals, what entitle us to conclusion, that it is particularly suitable for real-time computations.

References

[1] Y.B. AHN and S.B. PARK, *Estimation of mean frequency and variance of ultrasonic Doppler signal by using second-order autoregressive model*, IEEE Trans. on Ultrasonics, Ferroelectric and Frequency Control, **38**, 172–182, (1991).

[2] H. AKAIKE, *A new look at the statisticsl model identification*, IEEE Trans. Autom. Control, **19**, 716–723 (1974).

[3] B. ANGELSEN, *Theoretical study of scattering of ultrasound from blood*, IEEE Trans. BME, **27**, 61–67, (1980).

[4] B. AANGELSEN, *Instantaneous frequency, mean frequency and variance of mean frequency estimators for ultrasonic blood velocity Doppler signals*, IEEE Trans. BME, **28**, 733–741, (1981).
[5] P. ATKINSON and J.P. WOODCOCK, *Doppler ultrasound and its use in clinical measurement*, Academic Press, New York, (1982).
[6] M. AZIMI and A.C. KAK, *An analytical study of Doppler ultrasound systems*, Ultrason. Imaging, **7**, 1–48, (1985).
[7] W. BRODY and I. MEINDEL, *Theoretical analysis of the C.W. Doppler ultrasonic flowmeter*, IEEE Trans. BME, **21**, 183–192, (1974).
[8] J.P. BURG, *A new analysis technique for time series data*, NATO Advanced Study Inst. on Signal Processing Conf, (1968).
[9] J.P. BURG, *Maximum entropy spectral analysis*, Proc. of the 37th Meeting of the Society of Exploration Geophysics, (1967).
[10] J.A. CADZOW, *High performance spectral estimation — a new ARMA method*, IEEE Trans. ASSP, **28**, 524–529, (1980).
[11] J.A. CADZOW, *Spectral estimation: an overdetermined rational model equation approach*, IEEE Proc., **70**, 907–939, (1982).
[12] T. D'ALESSIO T., *Objective algorithm for maximum frequency estimation in Doppler spectral analysers*, Med. Biol. Engng and Comput., **23**, 63–68, (1985).
[13] R.J. DOVIAK and D.S. ZRNIC, *Doppler radar and weather observations*, Academic Press Inc., (1984).
[14] K.W. FERRARA and V.R. ALGAZI, *A new wideband spread target maximum likelihood estimator for blood velocity estimation-part 1: Theory*, IEEE Trans, Ultrason. Ferroelec. Freq. Contr., **38**, 17–26, (1991).
[15] L.L. FOLDY, *The multiple scattering of waves*, Phys. Rev, **67**, 107–119, (1945).
[16] S. HOLLAND, *Estimation of blood flow parameters using pulse Doppler ultrasound with corrections for spectral broadening*, Ph. D. Dissertation, Yale Univ., New Haven, CT, UMI Dissertation Information Service, (1987).
[17] L. HATLE and B. ANGELSEN, *Doppler ultrasound in cardiology. Physical principles and clinical applications*, Lea & Febriger, Philadelphia, (1987).
[18] K. KAŁUŻYŃSKI, *Selection of spectral analysis method for the assessment of velocity distribution based on the spectral distribution of ultrasonic Doppler signal*, Medical & Biological Engineering & Computing, **27**, 463–469, (1989).
[19] S.M. KAY and S.L. MARPLE, *Spectrum analysis — a modern perspective*, Proc. of IEEE, **69**, 1380–1419, (1981).
[20] S.M. KAY, *Modern spectral estimation:* Theory and application, Prentice Hall, Englewood Cliffs, New Jersey, (1988).
[21] M. LAX, *Multiple scattering of waves*, II; *The effective field in dese systems*, Phys. Rev., **85**, 261–269, (1952).
[22] A. MIHRAM, *Simulation, statistical foundation and methodology*, Academic Press, Inc., New York, (1972).
[23] L. MO, L.C. YUN, R. COBBOLD, *Comparison of four digital maximum frequency estimators for Doppler ultrasound*, Ultrasound in Med. & Biol, **14**, 355–365, (1988).
[24] L. MO and R. COBBOLD, *A stochastic model of the backscattered Doppler ultrasound from blood*, IEEE Trans. BME, **33**, 20–27, (1986).
[25] A. NOWICKI, P. KARLOWICZ, M. PIECHOCKI and W. SECOMSKI, *Method for the measurement of the maximum Doppler frequency*. Ultrasound in Med. & Biol, **11**, 479–486, (1985).
[26] A. PAPOULIS, *Probality, random variables and stochastic processes*, McGrow–Hill Inc., (1965).
[27] I.S. REED, D.W. TUFTS, X. YU, T.K. TRUONG, M.T. SHIH, X. YIN, *Fourier analysis and signal processing by use of the Mobius inversion formula*, IEEE Trans. ASSP, **38**, 458–470, (1990).
[28] A. SAINZ, V.C. ROBERTS and G. PINARDI, *Phase-locked loop techniques applied to ultrasonic Doppler signal processing*, Ultrasonics, **14**, 128–132, (1976).
[29] F. SCHLINDWEIN, D.H. EVANS, *Selection of the order of autoregressive models for spectral analysis of Doppler Ultrasound signals*, Ultrasound in Med. & Biol., **28**, 81–91, (1990).

[30] K.K. SHUNG, R.A. SIGELMANN and J.M. REID, *Scattering of ultrasound by blood*, IEEE Trans. BME, **23**, 460–467, (1976).

[31] D. SIRMANS and B. BUMGARNER, *Numerical comparison of five mean frequency estimators*, J. Applied Meteorology, **14**, 991–1003, (1975).

[32] M.I. SKOLNIK, *Introduction to radar systems*, McGraw–Hill Book Comp. Inc., New York, (1962).

[33] P. STOICA, T. SODERSTROM, *Optimal instrumental variable estimation and approximate implementation*, IEEE Trans. Autom. Control, **28**, 757–772, (1983).

[34] D.N. SWINGLER, *Frequency estimation variance with the Burg algorithm*, IEEE Trans. SP, **39**, 1003–1005 (1991).

[35] N. TEPEDELENLIOGLIOU, *A note on the computational complexity of the arithmetic Fourier transform*, IEEE Trans. ASSP, **37**, 1146–1147, (1989).

[36] V. TWERSKY, *On scattering of waves by random distribution-I: Freespace scatterer formalism*, J. Math. Phys., **3**, 700–704, (1962).

[37] P.J. VAITKUS and R. COBBOLD, *A comparative study and assessment of Doppler ultrasound spectral estimation technques*, Part I: *Estimation methods*, Ultrasound in Med. & Biol, **14**, 661–672, (1988).

[38] P.J. VAITKUS, R. COBBOLD, K.W. JOHNSTON, *A comparative study and assessment of Doppler ultrasound spectral estimation techniques, Part II: Methods and results*, Ultrasound in Med. & Biol, **14**, 673–688, (1988).